



DFT Computational Study of the Epoxidation of Olefins with Dioxiranes

Mauro Freccero^a, Remo Gandolfi^a, Mirko Sarzi-Amadè^{a*}, Augusto Rastelli^b

^aDipartimento di Chimica Organica, Università di Pavia, V.le Taramelli 10, 27100 Pavia Italy.

^bDipartimento di Chimica, Università di Modena, Via Campi 183, 41100 Modena, Italy.

Received 19 February 1998; revised 30 March 1998; accepted 2 April 1998

Abstract: transition structures (TSs) of the reactions of dioxirane and dimethyldioxirane with ethylene, propene, cis-2-butene and trans-2-butene were located with the B3LYP/6-31G* method. The TSs of the reactions of ethylene and cis-2-butene exhibit a symmetrical spiro butterfly structure with synchronous formation of the two new C–O bonds and with substantial alignment of π bond axis with the breaking O–O bond. In the case of propene and trans-2-butene a slight asynchrony in C–O bond formation was predicted by calculations. Theoretical activation free enthalpies (gas phase) reproduce the experimental (acetone solution) higher reactivity of cis with respect to trans disubstituted alkenes which in turn are correctly predicted more reactive than monosubstituted alkenes. Also the calculated absolute activation free enthalpies, after correction for electrostatic solvation effects by single point SCRF calculation (Tomasi model), were found to be in reasonable accord with experimental data. © 1998 Elsevier Science Ltd. All rights reserved.

Keywords: Dioxiranes; Epoxidation; Transition states

INTRODUCTION

In the last few years dioxiranes^{1–4}, particularly dimethyldioxirane (DMD)^{5–8}, have progressively become popular reagents among synthetic organic chemists for their high reactivity in oxidation reactions. In particular, they are widely used in epoxidation reaction of alkenes because of mild reaction conditions and easy workup. Experimental investigations dealing with the mechanism of the oxygen atom transfer^{9,10} were obviously stimulated by the synthetic usefulness of these reactions but only recently there has also been a growing interest in computationally addressing the mechanistic aspects of dioxirane oxidations which seem to closely parallel those of peroxyacid oxidations.

In this paper we will report our computational results on the mechanism of epoxidation of simple alkenes (ethylene, propene, cis and trans-2-butene) with both the parent dioxirane (DHD) and DMD.

Kinetic studies by Baumstark et al.¹⁰ have shown that cis-alkenes exhibit a definitely higher reactivity than trans-alkenes in their reaction with DMD. This finding led the above authors to advance for the transition state (TS) of these reactions a “spiro” butterfly structure which should benefit from less steric interaction than its “planar” butterfly counterpart (Figure 1). In fact, in the spiro-TSs of DMD oxidations of trans-olefins there is an unfavorable steric interaction between one of the alkyl groups of the trans-olefin and one of the methyl groups of the dioxirane moiety while such an interaction is missing in the exo spiro-TSs of cis-olefins. This observation explains the higher reactivity of the latter. By contrast, similar repulsive steric interactions are at work in planar-TSs for the reactions of both cis- and trans-olefins.

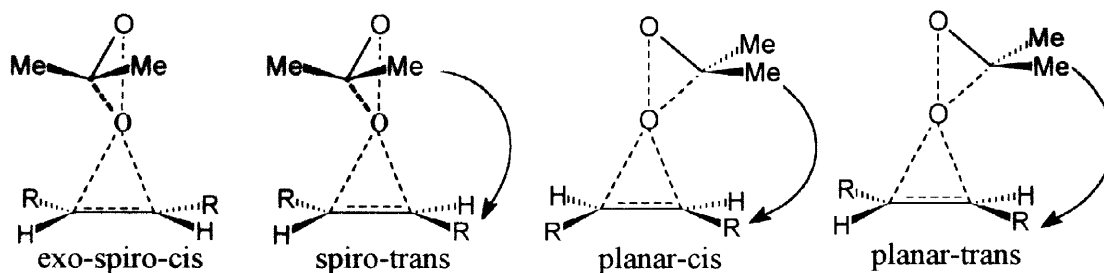


Figure 1. Spiro and planar transition states of the epoxidation reaction of cis- and trans-olefins with dimethyldioxirane.

Baumstark et al.¹⁰ suggested that there can be competition between spiro and planar TSs as “the energy difference between the two extremes TSs is small enough to be overcome”. Moreover, very recently, in the context of a study of an asymmetric epoxidation,¹¹ the spiro-TS led itself as the more suitable model to correctly predict the stereochemistry of the dominant enantiomer but a planar TS seemed to be operative as main competing pathway.

A spiro-TS with dipolar character (alkene acting as a donor, and dioxirane as an acceptor through a π - σ^* interaction) seems to be well suited to explain intramolecular hydrogen bonding effect observed in the case of the reaction of DMD with both cyclic and acyclic allylic alcohols^{12–15} as well as the increase in epoxidation rate in the presence of hydrogen bond donor cosolvent such as water or methanol¹⁶ (Figure 2). Intramolecular effects, which increase face selectivity, are highest in non polar solvents such as CCl_4 which can not act either as hydrogen bond acceptor or as hydrogen bond donor.

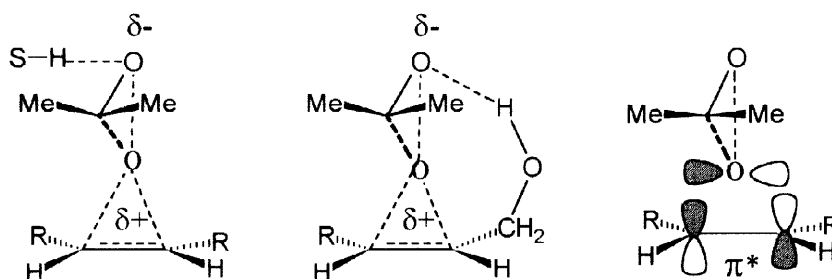


Figure 2. Solvent hydrogen bonding interaction and intramolecular hydrogen bonding for acyclic allylic alcohols. Back donation through the π^* - $p_{\text{lone pair}}$ interaction in the spiro transition structure.

On the theoretical side, calculations concerning dioxirane structure have been carried out by Kraka^{17,18} and co-workers while the reaction of dioxiranes with amines has been investigated by Miaskiewicz.¹⁹ At the beginning of our study the only reported fully optimized transition structure (TS) of epoxidation reaction with dioxiranes was that of the reaction between the parent dioxirane (DHD) and ethylene at the MP2/6-31G* level of theory²⁰ and of DMD and ethylene at the HF/6-31G* level.²⁰ The former TS exhibits a spiro-like structure with a quite asynchronous formation of the two new carbon oxygen bonds (1.820 Å vs 2.330 Å) while the spiro structure of the latter is synchronous.

There is a general agreement that HF wave functions are not adequate to properly describe the potential energy surface of dioxirane reactions and only correlated calculations can provide reliable geometries and energies of TSs of these reactions. Some years ago it was suggested that calculations with introduction of dynamic correlation at the lowest Moeller-Plesset level (MP2) can be confidently used in geometry optimization of dioxirane reactions while energies have to be computed at higher level to obtain reasonably safe calculated barriers (MP4/6-31G**/MP2/6-31G*²⁰).

Thus, on the basis of this suggestion one has to have confidence in the asynchronous TS of the reaction of ethylene with DHD at the MP2/6-31G* level and to consider with some reservation the synchronous HF TS of the reaction of dimethyldioxirane with ethylene.

However, very recently Singleton, Houk et al.²¹ showed that the MP2/6-31G* method predicts, as found before by other authors,²¹⁻²³ an asynchronous TS for the reaction of peroxyformic acid with ethylene [it is amusing to realize that asynchrony in carbon-oxygen bond formation in the TS of this reaction (1.805 Å vs 2.263 Å) mimics in an astonishing way that one of the reaction of DHD with ethylene (see above)] whereas DFT theory at the Becke3-LYP/6-31G* level predicts a perfectly synchronous (as for the two incipient CO bonds) TS. These authors also demonstrated that the latter geometry and the related vibrational frequencies provide a superior description of the ¹H secondary and ¹³C primary kinetic isotope effect as they indicate a perfect match to the experimental data.

The latter results cast serious doubt on the TS “asynchrony” predicted by the MP2/6-31G* method for the reaction of DHD with ethylene thus leaving open the problem of the prototype geometry for transition structures of dioxirane epoxidation.

This led us, in the context of an experimental and theoretical study directed to assess the factors that control face selectivity in epoxidation of plane non symmetric double bonds (of cis-3,4-disubstituted cyclobutenes²⁴ and cis,exo-5,6-disubstituted bicyclo[2.2.2]oct-2-enes²⁵) with peroxyacids and dioxiranes, to reinvestigate the transition structures of the reactions of DHD and DMD (Figure 3) with ethylene. We aimed at defining the intrinsic characteristics of the TSs of these reactions and, in particular, the degree of asynchrony in CO bond formation as well as the relative energies of spiro vs planar butterfly structures. We chose the DFT theory as this method seems to emerge as the method of choice for a reliable description of the energetics of organic reactions at a reasonable cost. We extended our investigation to the reaction of DHD and of DMD with an unsymmetrically substituted alkene (propene) as well as with cis- and trans-2-butene (Scheme 1) in order to assess to what extent moderate unsymmetry of the alkene is reflected in the TS and to what extent steric interactions can change the TS geometry. Moreover, a comparison between the calculated activation energies of these latter reactions and the known experimental values¹⁰ of the reactions of DMD with 1-nonene and cis- and trans-3-hexenes offers the appealing opportunity to safely evaluate the reliability of the DFT calculations in reproducing reactivity data (both absolute and relative values) in dioxirane epoxidation reactions.

The publication of two papers on the same issue by Houk et al. prompts us to publish our own results.^{26,27}

COMPUTATIONAL METHODS

The energies (Table 1) and geometries (Table 2) of the educts as well as of the transition structures [TSs] were calculated with density functional theory (DFT) using the Becke3-LYP functional^{28,29} and the 6-31G* basis set. All calculation were performed with the Gaussian 94 suite of programs³⁰. Critical points have been characterized by diagonalizing the Hessian matrices calculated for the optimized structures; transition structures have only one negative eigenvalue (first order saddle points) with the corresponding eigenvector involving the expected formation of the two new oxirane bonds and cleavage of the O₃O₄ and C₅O₃ dioxirane bonds. The transition mode imaginary frequencies (cm⁻¹) of the TSs are reported in Table 2. The search for TSs was limited to concerted transition structure.²⁶

In order to produce theoretical activation parameters, vibrational frequencies in the harmonic approximation were calculated for all the optimized B3LYP/6-31G* structures and used, unscaled,³¹ to compute the zero point energies, their thermal corrections, the vibrational entropies, and their contributions to activation enthalpies, entropies and free enthalpies (Tables 1 and 3).

The contribution of solvent effects to the activation free enthalpy of the reactions under study are calculated via the self-consistent reaction field (SCRF) using the Tomasi model (interlocking spheres) by single point calculations (i.e., with unrelaxed gas-phase geometries of reactants and TSs) at the B3LYP/6-31G* level (Table 4).³²⁻³⁵

Cartesian coordinates of all TSs are available on request.

Table 1. Electronic energies (hartree), electronic activation energies and computed kinetic contributions to the thermodynamic properties (at 298K) of reactants and transition structures for the dioxirane reactions.^a

Structures	Energies	ΔE^\ddagger	ZPE	δH	S	δG	$\delta \Delta H^\ddagger$	ΔS^\ddagger	$\delta \Delta G^\ddagger$
Ethylene	-78.587457		32.14	34.64	52.32	19.04			
Propene	-117.907556		50.24	53.40	63.22	34.55			
Cis-2-Butene	-157.224767		68.18	72.21	70.60	51.16			
Trans-2-butene	-157.226904		68.06	72.09	69.82	51.27			
DHD	-189.615552		20.52	23.01	57.47	5.88			
DMD	-268.268944		55.68	59.79	71.82	38.37			
1a	-268.182377	12.94	53.51	57.97	78.01	34.71	0.32	-31.78	9.79
2a	-307.505723	10.91	71.30	76.65	85.22	51.24	0.24	-35.47	10.81
3a	-307.504571	11.63	71.37	76.66	84.33	51.52	0.25	-36.36	11.09
4a	-346.826174	8.88	89.03	95.40	93.84	67.43	0.18	-34.24	10.39
5a	-346.823555	10.52	89.19	95.41	91.82	68.03	0.19	-36.25	10.99
6a	-346.826693	9.89	89.02	95.29	92.03	67.85	0.19	-35.27	10.70
1b	-346.827906	17.88	88.52	94.66	90.17	67.76	0.23	-33.97	10.35
2b	-386.151167	15.90	106.33	113.36	97.63	84.25	0.17	-37.41	11.33
3b	-386.149303	17.07	106.43	113.37	96.37	84.64	0.18	-38.68	11.72
4b	-425.471633	13.85	123.97	132.05	106.28	100.36	0.05	-36.15	10.83
6b	-425.471153	15.50	124.06	131.97	103.62	101.08	0.09	-38.03	11.44

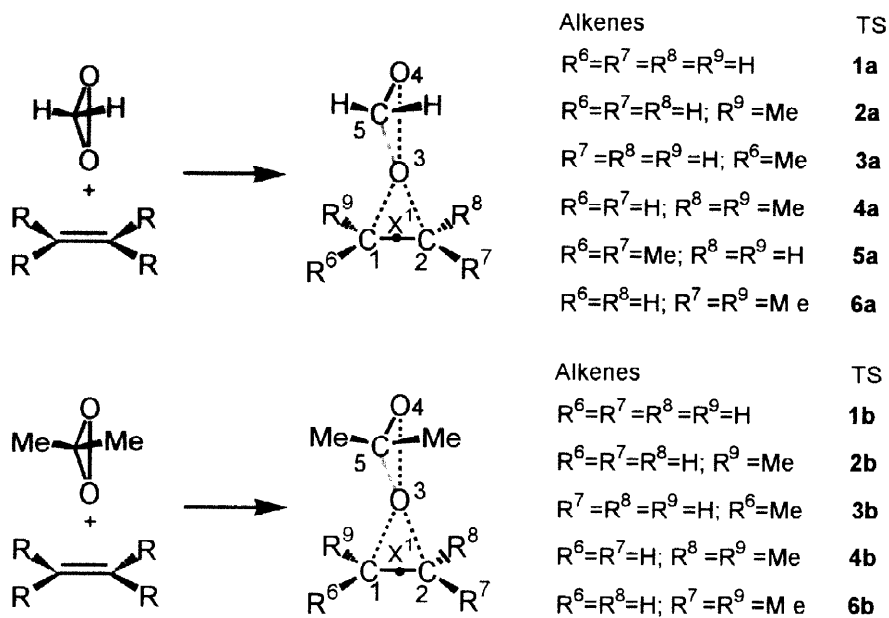
^aHarmonic approximation assumed; standard state (298K) of the fugacity scale (pure perfect gas at 1 atm); energies in kcal mol⁻¹ and entropies in e.u. (cal/mol K); ΔE^\ddagger : electronic activation energies; ZPE: zero point energy; δH , δG are the kinetic contributions to molar enthalpy and free enthalpy (to be added to electronic energy); S is the molar entropy; $\delta \Delta H^\ddagger$ and $\delta \Delta G^\ddagger$ are the kinetic contributions to molar activation enthalpy and free enthalpy; ΔS^\ddagger is the molar activation entropy. Symmetry numbers used to calculate entropy are $\sigma = 4$ for ethylene, $\sigma = 2$ for cis-, trans-2-butene and dioxiranes, $\sigma = 1$ for propene and all the transition structures.

RESULTS AND DISCUSSION

Transition structures for the epoxidation of ethylene

The TS of the reaction of the parent dioxirane with ethylene, i.e. **1a**, is reported in Figure 3. As found by Bach et al. at the MP2/6-31G* level²³ the alkene fragment has only slightly been perturbed as shown by the small stretching of the double bond (by only 0.04 Å) as well as the low out-of-plane distortion of the olefinic hydrogens (dihedral angles between the two planes H₆-C₁-C₂-H₇ and H₉-C₁-C₂-H₈ = 5.2°).

The most significant geometry distortion of the former dioxirane in TS **1a** is a substantial lengthening (by 0.37 Å) of the O₃O₄ peroxy bond whereas the weakening of the other bond that will break, i.e. O₃C₅, is only at its beginning. Furthermore, the C₅O₄ bond is just slightly shorter (by 0.04 Å) than in dioxirane itself and there is no appreciable flattening of the tetrahedral C₅. On the basis of these geometry data we can conclude that the high reactivity of dioxiranes benefits more from relief of the three-membered ring strain than from formation of the strong carbonyl bond.



Scheme 1

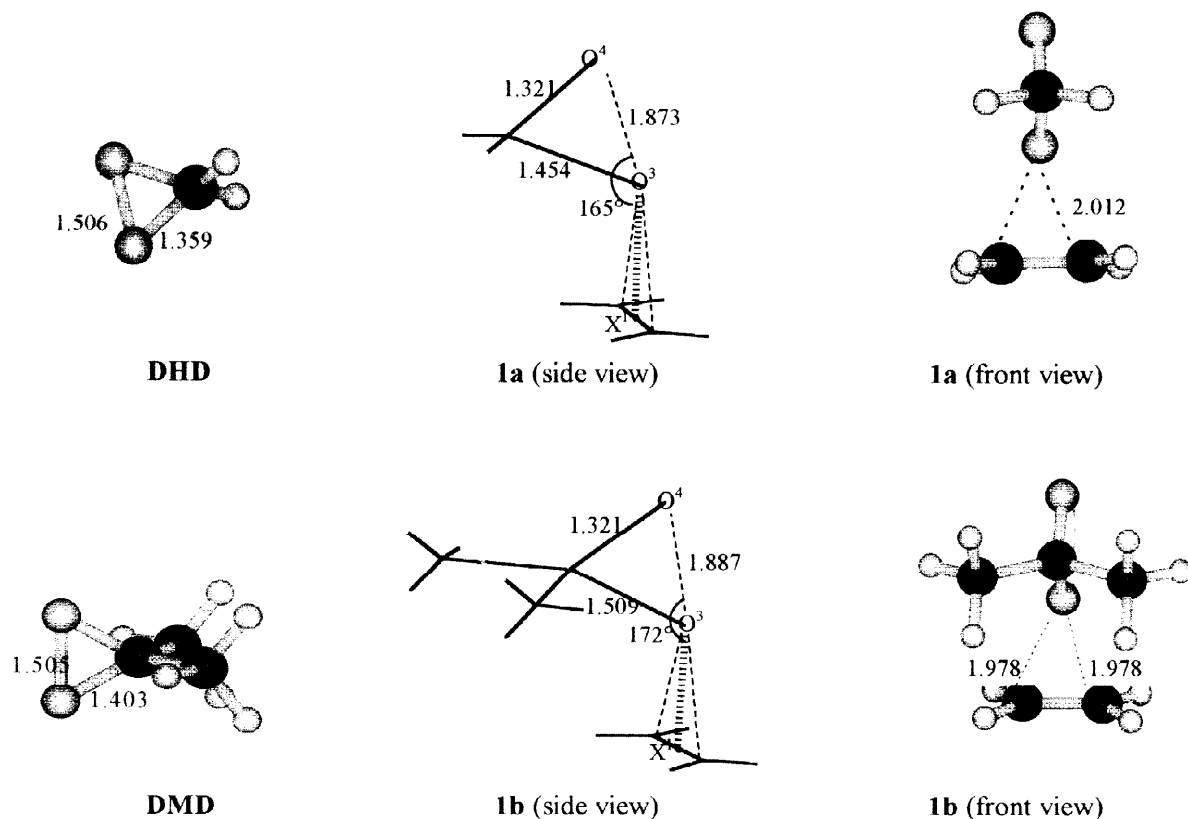


Figure 3. DHD and DMD structures. TSs of DHD and DMD reactions with ethylene (**1a** and **1b**, respectively). Bond lengths in angstroms.

Table 2. Bond lengths^a (Angstroms), dipole moments^b (Debye) and transition mode imaginary frequencies (cm⁻¹) of TSs 1-6.

Parameter	1a	2a	3a	4a	5a	6a
O ₃ -O ₄	1.873	1.860	1.870	1.860	1.879	1.866
O ₃ -C ₅	1.454	1.445	1.444	1.437	1.447	1.441
C ₅ -O ₄	1.321	1.325	1.326	1.329	1.325	1.327
C ₁ -C ₂	1.370	1.372	1.372	1.376	1.378	1.374
μ	4.86	5.06	5.29	5.10	5.62	5.26
transition mode	463.5	430.9	440.1	394.8	414.9	409.7
Parameter	1b	2b	3b	4b	6b	
O ₃ -O ₄	1.887	1.880	1.883	1.884	1.883	
O ₃ -C ₅	1.509	1.495	1.497	1.485	1.494	
C ₅ -O ₄	1.321	1.320	1.325	1.327	1.325	
C ₁ -C ₂	1.374	1.375	1.378	1.380	1.378	
μ	4.53	4.76	4.94	4.84	4.88	
transition mode	535.8	500.1	501.3	466.7	479.7	

^a Double bond length: ethylene = 1.331 Å; propene = 1.333 Å; cis-2-butene = 1.338 Å; trans-2-butene = 1.335 Å.

^b Dipole moment: dioxirane, μ = 2.53 D; dimethyldioxirane, μ = 2.89 D; propene, μ = 0.36 D; cis-2-butene, μ = 0.18 D.

The B3LYP/6-31G* TS differs significantly from that obtained at the MP2/6-31G* level: the former, at variance with the pronounced asynchrony of the latter, exhibits perfect synchrony in the formation of the two CO bonds (2.012 Å). The TS **1a** features a spiro butterfly structure with a 90° angle between the plane of the three-membered dioxirane ring (O₃C₅O₄) and the ethylene CC double bond. Notice also that the forming oxirane plane (C₁O₃C₂) is almost symmetrically disposed with respect to the ethylene moiety (i.e., the dihedral angle between this plane and H₉C₁C₂H₈ is 94° while that with H₆C₁C₂H₇ is 89°). Moreover, the breaking peroxide bond (O₃O₄) is almost aligned with the π axis of the ethylene double bond (X₁Ö₃O₄ angle = 165°; X₁ is a dummy atom placed at the center of C₁C₂ bonds). Thus, DFT calculations suggest an S_N2 like alignment between the nucleophilic π bond and the electrophilic OO bond. However, the small deviation of the X₁Ö₃O₄ angle from 180° (it is present in all TSs 1-6) is certainly the result of an electronic effect as it gives rise to increase in steric congestion (i.e., the HC₃H moiety bends towards the endo ethylene hydrogens) and can be traced back to the tendency to improve orbital interaction as far as possible.

The TS of the reaction of DHD with ethylene shares with that of peroxyformic acid epoxidation of the same substrate^{21,36} the synchronous spiro butterfly structure. This structure seems to be intrinsically favored over an asynchronous TS and over what is indicated as a planar structure (see Figure 1). We unsuccessfully tried to locate either an asynchronous spiro or a planar transition structure. These TSs seem not to be first order saddle points on the potential energy surface. In fact, the frequency calculation on a constrained planar structure for the reaction of DHD with ethylene showed the presence of two negative eigenvalues (second order saddle point) with the eigenvector corresponding to the second negative eigenvalue involving rotation of the dioxirane moiety from the planar to the spiro orientation.

In qualitative terms, the favor for the spiro structure can be attributed to back donation (from dioxirane to CC double bond) involving a p lone pair of the proximal oxygen of the dioxirane (i.e., O₃) and the π* of the CC double bond while the p lone pair of the distal oxygen atom (i.e., O₄) is ideally oriented to provide electron density for hydrogen bonding interaction with an allylic OH group³⁷ or with a solvent molecule. These interactions are schematically represented in Figure 2. Moreover, torsional interactions disfavor the planar

structure: staggering between the bonds of the attacking dioxirane and of ethylene is certainly worse in a planar TS than in its spiro counterpart. We conclude that in dioxirane epoxidation a spiro TS is definitely more stable than a planar TS and that this energy difference cannot easily be overcome.

Introduction of two methyl groups in the dioxirane (i.e. on passing from DHD to DMD) does not significantly alter the TS geometry of the reaction with ethylene. Once again the TS, i.e. **1b** in Figure 3, shows a spiro array of the two three-membered rings with a dihedral angle between the $O_3C_5O_4$ plane and the average alkene plane of $\approx 90^\circ$ (put in other words the angle between the $O_3C_5O_4$ plane and the C=C bond axis is 90°). Incipient C–O bond lengths in the forming oxirane ring of **1b** are equal and slightly shorter (by 0.03 Å) than in TS **1a** of the DHD reaction.

Geometry characteristics (in particular bond lengthening and shortening of the dioxirane moiety as well as the small out-of-plane distortion of the alkene substituents) of the former educt moieties in **1b** are very similar to those commented above for **1a** and Table 2 (where selected geometrical details are reported) clearly shows that this observation holds for all the TSs investigated by us.

The O_3O_4 bond distance in **1b** (1.887 Å) is slightly shorter than that (2.011 Å) of the TS of the oxidation of methylamine by DMD¹⁹. That is, a strong increase in nucleophilicity on passing from ethylene to methylamine is reflected in a relatively small lengthening of the O_3O_4 bond in the TS. This observation is consistent with the finding that the very small increase in nucleophilicity of a double bond as a result of introducing methyl groups on it (i.e., on going from ethylene to propene and 2-butenes) does not bring about any significant change either in the O_3O_4 bond length (Table 2) or in the amount of charge transfer (see below) from the nucleophilic alkene to the electrophilic dioxirane.

Synchronous bond formation in a spiro TS has also been found at the HF/6-31G* for the reaction of DMD with ethylene.²⁰ However, the DFT structure differs in important details from the Hartree-Fock one: C–O forming bond lengths are substantially longer (by 0.51 Å) in the latter TS than in the former one. Moreover, the leading geometry change of the HF TS is represented not only by breaking of the O_3O_4 bond (1.870 Å), as in DFT TS, but also by the breaking process of the C_5O_3 bond (2.008 Å) and formation of the C_5O_4 double bond (1.221 Å) while the flattening of C_5 is here almost complete.

Transition structures for the epoxidation of propene and cis- and trans-2-butene

The methyl group in propene induces a small electronic polarization of the double bond which can be held responsible of the small but significant amount of asynchrony in the exo TSs (i.e. **2**): the incipient CO bonds in both **2a** and **2b** differ by 0.15 Å (Figure 4). In the endo TS **3** steric effects cooperate in increasing asynchrony which is now sizable: in **3b** the difference in CO forming bond lengths is of 0.318 Å while in the less crowded **3a** this difference is reduced to 0.236 Å. However, it should be stressed that “asynchrony” predicted by DFT calculations for a TS which “must” be asynchronous is much smaller than that predicted by MP2/6-31G* calculations (0.510 Å, see above) for the TS of the reaction of the DHD with ethylene. The above observation is in order to emphasize that MP2/6-31G* is definitely biased against synchronous TSs in epoxidation reactions. Asynchrony in bond formation is accompanied by $O_3C_5O_4$ plane tilting, with respect to a perpendicular orientation to the C=C bond axis, by 5° in **2b** and by 17° in **3b**. Geometry deformations of the endo TSs **3** induced by steric interactions in comparison to the “ideal” structure represented by the exo TSs **2** are not energetically very expensive: the endo TS **3b** (**3a**) is predicted to be less stable than the exo TS **2b** (**2a**) by 1.56 (1.00) kcal mol⁻¹ in gas phase (Table 3) and 1.74 (0.73) kcal mol⁻¹ in acetone solution ($\epsilon = 21$) when electrostatic solvation effects are introduced by single point SCRF calculations (Tomasi model)³²⁻³⁵ (Table 4).

The geometries of the transition structures of the reactions of DMD with cis- and trans-2-butene closely resemble those found for the reactions with ethylene and propene (Figure 5). In the case of the reaction of cis-2-butene with DMD only the exo TS **4b** was investigated by us as its endo counterpart should be less stable by > 3 kcal mol⁻¹ (with practically no contribution to the reaction rate of this alkene), as suggested by the relative energies of **2b** and **3b**. Moreover, the endo TS **5a** from DHD is already 2.24 kcal mol⁻¹ less stable than its exo diastereoisomer **4a** in the gas phase (Table 3). The inclusion of solvent effect halves this difference to 1.12 kcal mol⁻¹ (Table 4).

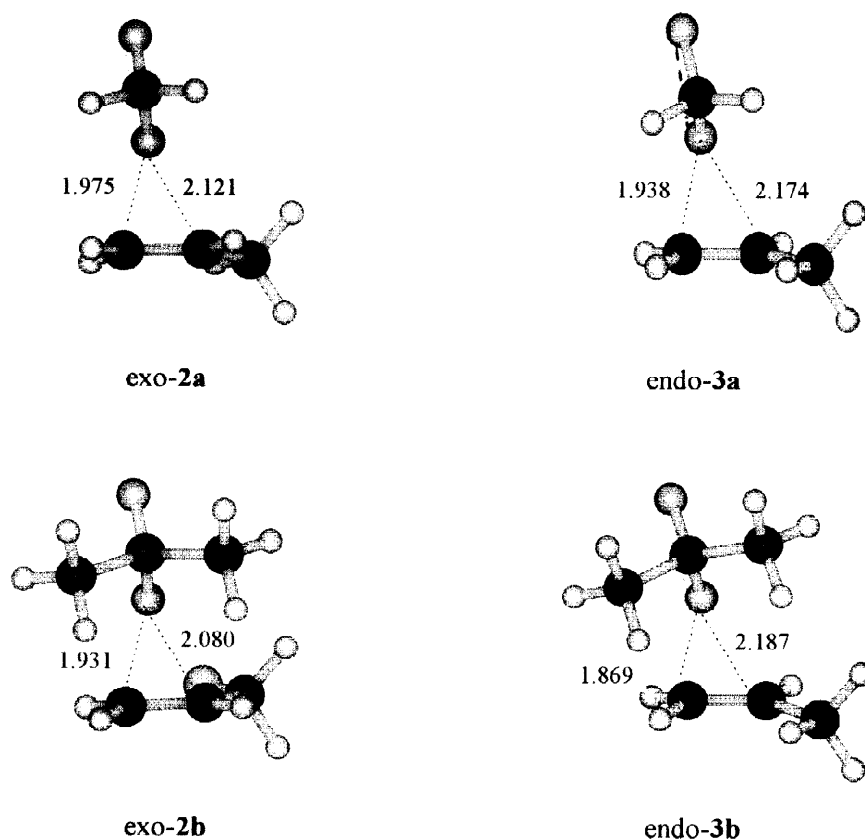


Figure 4. TSs for the reaction of DHD and DMD with propene (**2a**, **3a** and **2b**, **3b** respectively). Bond lengths in angstroms. In exo (endo) TSs the substituents on dioxirane are on the opposite (same) side with respect to substituents on alkene.

The geometry of the spiro synchronous exo TSs **4** from cis-2-butene, with incipient CO lengths (2.074 Å in **4a** and 2.026 Å in **4b**) only slightly longer than those of **1** and the forming oxirane plane symmetrically disposed (dihedral angles: C₁O₃C₂ plane/ H₆C₁C₂H₇ plane and C₁O₃C₂ plane/ CC₁C₂C plane ≈ 93° both in **4a** and **4b**) needs no detailed comment. In TS **5a** the plane of the forming oxirane ring rotates away from the methyl groups (dihedral angles: C₁O₃C₂ plane/ H₆C₁C₂H₇ plane ≈ 86° and C₁O₃C₂ plane/ CC₁C₂C plane ≈ 102°) in order to alleviate steric congestion while the X₁O₃O₄ angle remains unaltered on going from **4a** (166°) to **5a** (167°).

The asynchrony of TS **6b** from trans-2-butene (Figure 5) is more similar to that of the endo TS **3b** (controlled by electronic plus steric effects) than to that of the exo TS **2b** (dictated only by double bond polarization). In **6b** only steric effects are at work but these interactions (methyl-methyl interaction) promote a considerable difference in forming bond lengths (0.205 Å) and a tilting of the O₃C₃O₄ plane by 14° with respect to perpendicular orientation. In **6a** asynchrony, controlled by small steric effects, is only 0.087 Å.

ACTIVATION FREE ENTHALPY

And now the usual question: to what extent do the computational data reproduce experimental absolute and relative reaction rates?

The second-order reaction rates of the reaction of cis-3-hexene, trans-3-hexene and 1-nonene with DMD were carefully measured by Baumstark et al.¹⁰ in acetone at 25°C (k=0.57, 0.067, and 0.035 L⁻¹ mol s⁻¹, respectively).

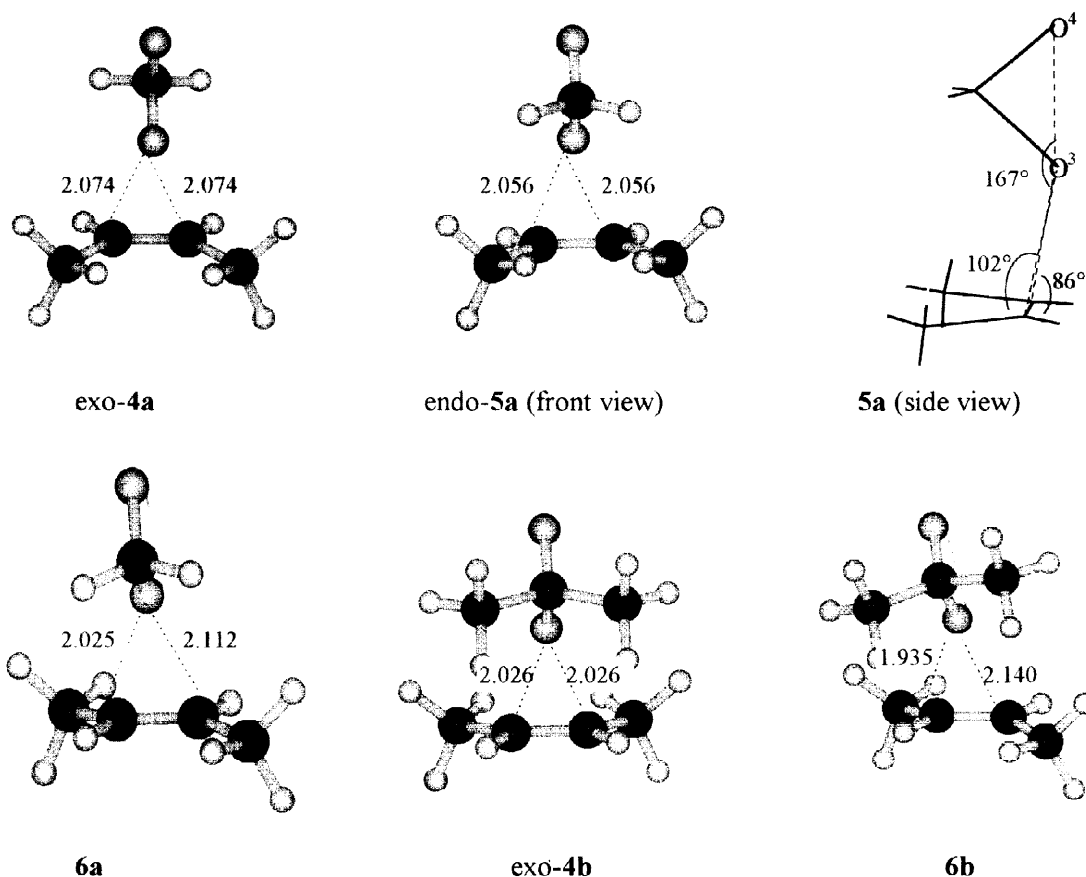


Figure 5. TSs of the reaction of DHD and DMD with *cis*-2-butene and *trans*-2-butene (**4a**, **5a**, **6a**, and **4b**, **6b**, respectively). Bond lengths in angstroms.

The corresponding activation free energies are as follows: $\Delta G_{\text{exp}}^{\ddagger} = 17.65$, 18.91 and 19.29 kcal mol⁻¹ for *cis*-3-hexene, *trans*-3-hexene and 1-nonene, respectively. We believe that the reactions of DMD with *cis*-2-butene, *trans*-2-butene and propene are satisfactory computational models to be profitably compared to these experimental reactions.

Calculated ΔH^{\ddagger} , ΔS^{\ddagger} and ΔG^{\ddagger} (gas phase) are reported in Table 3. Inspection of these data makes it evident that the relative gas phase activation free enthalpies ($\Delta\Delta G^{\ddagger} = 0.0$, 1.85 and 2.10 kcal mol⁻¹ for *cis*-2-butene, *trans*-2-butene and propene) are reasonably consistent with experimental data (acetone solution, $\Delta\Delta G_{\text{exp}}^{\ddagger} = 0.0$, 1.2 and 1.6 kcal mol⁻¹ for *cis*-3-hexene, *trans*-3-hexene and 1-nonene). In particular the higher reactivity of *cis* with respect to *trans* disubstituted alkenes is correctly predicted by calculations. The reaction rate order for these three substrates is also correctly reproduced by the relative electronic activation energies ($\Delta\Delta E^{\ddagger} = 0.0$, 1.65 and 3.22 kcal mol⁻¹ for *cis*-2-butene, *trans*-2-butene and propene).

Comparison between the absolute values shows that theoretical gas phase ΔG^{\ddagger} values are higher than the experimental data ($\Delta G_{\text{exp}}^{\ddagger}$) (acetone solution) by ≈ 5 kcal mol⁻¹. However, it should be emphasized that there is a strong increase in dipole moment on going from the educts (e.g., $\mu = 2.89$ D for DMD and 0.36 D for *cis*-2-butene) to TSs (e.g., $\mu = 4.84$ D for **4b**), which increase is similar in all of the reactions studied. The latter observation tells us that the relative activation free enthalpies should be only slightly influenced by electrostatic solvation effects but if we want to compare theoretical and experimental absolute values we cannot neglect these effects. Indeed, evaluation of solvent effects via the self-consistent reaction field (SCRF) using the Tomasi model (interlocking spheres) by single point calculations at the B3LYP/6-31G* level (acetone dielectric constant, $\epsilon = 21$) led to a stabilization of TSs with respect to educts of ≈ 6 kcal/mol (Table 4).

Table 3. Calculated activation parameters (at 298K) for transition structures 1-6 at the B3LYP/6-31G* level^a.

TS	ΔE^\ddagger	ΔH^\ddagger	ΔS^\ddagger	ΔG^\ddagger	$\Delta\Delta G^\ddagger$
1a	12.94	13.85	-23.44	20.84	
2a	10.91	11.74	-25.76	19.42	
3a	11.63	12.47	-26.65	20.42	
4a	8.88	9.65	-25.90	17.38	
5a	10.52	11.30	-27.92	19.62	
6a	9.89	10.67	-25.55	18.29	
1b	17.88	18.70	-25.63	26.34	
2b	15.90	16.66	-27.70	24.93	2.10 ^b
3b	17.07	17.84	-28.96	26.49	
4b	13.85	14.49	-27.81	22.79	0.00
6b	15.50	16.18	-28.31	24.64	1.85

^aEnergies in kcal mol⁻¹, entropy in eu; standard state (298K) of the molar concentration scale (gas in ideal mixture at 1 mol/L, P = 1 atm); ΔE^\ddagger is the electronic activation energy; ΔH^\ddagger , ΔG^\ddagger are the molar enthalpy and free enthalpy, ΔS^\ddagger is the molar activation entropy. For conversion from 1 atm standard state (Table 1) to 1 mol/L standard state (both for gas phase) the following contributions need to be added to standard enthalpy, free enthalpy, and entropy, respectively: $-RT$, $RT \ln R^\ddagger T$, $-R \ln R^\ddagger T - R$, where R^\ddagger is the value of the R constant given in L atm/molK. For a reaction with A + B = C stoichiometry, the corrections for ΔH^\ddagger , ΔG^\ddagger and ΔS^\ddagger are RT , $-RT \ln R^\ddagger T$, $R \ln R^\ddagger T + R$. At 298 K the corrections amount to 0.59 and -1.90 kcal mol⁻¹ for ΔH^\ddagger and ΔG^\ddagger respectively and 8.34 eu for ΔS^\ddagger . A further correction of $R \ln 2$ to ΔS^\ddagger is added for the reactions of propene (both for exo and endo pathways) and of trans-2-butene as the attacks to their enantiopic faces are not experimentally distinguishable.

^bIn order to compare calculated with experimental ΔG^\ddagger in the case of the reaction of propene, calculation should take into account both the exo and endo pathway. This leads to $\Delta G^\ddagger = 24.89$ kcal mol⁻¹ for oxirane formation { i.e., $\Delta G^\ddagger = \Delta G_{\text{exo}}^\ddagger + RT \ln [1 + e^{(\Delta G_{\text{exo}}^\ddagger - \Delta G_{\text{endo}}^\ddagger)/RT}]$ }, which is not significantly different from $\Delta G_{\text{exo}}^\ddagger$.

The theoretical absolute activation free enthalpies, after correction with solvent effects, closely reproduce the experimental values ($\Delta G^\ddagger = 16.7$, 18.1 and 18.9 kcal mol⁻¹ for cis-2-butene, trans-2-butene and propene, respectively, vs $\Delta G_{\text{exp}}^\ddagger = 17.7$, 18.9 and 19.3 kcal mol⁻¹ for cis-3-hexene, trans-3-hexene and 1-nonene, respectively) while the relative values are left, as expected, substantially unaltered ($\Delta\Delta G^\ddagger = 0.0$, 1.4 and 2.2 kcal mol⁻¹, respectively).³⁹

Strong stabilization of the TS relative to starting reactants by solvent effect has been also reported by Miaskiewics et al. in the computational investigation of the reaction of methylamine with DMD.¹⁹ The increase in dipole moment on going from educts to TS in the epoxidation with dioxirane is certainly the result of electron density transfer from the nucleophilic alkene to the electrophilic dioxirane (via, in FO terms, the $\sigma_{\text{OO}}^* - \pi$ interaction). This amounts to ≈ 0.30 electrons (on the basis of Mulliken population analysis as well as on the basis of CHelpG charges) and increases almost negligibly on passing from ethylene to methyl-substituted derivatives. In the TSs the negative atomic net charge on O₄ (≈ -0.50) is significantly higher than that on O₃ (≈ -0.30). Actually, this latter is very similar to that present in the starting dioxirane so that electron density transferred from alkene to dioxirane is mostly localized on the distal oxygen atom O₄.

Kinetic studies at variable temperature allowed Murray et al.¹⁶ to evaluate the activation enthalpy ($\Delta H^\ddagger = 7.4 \pm 0.3$ kcal mol⁻¹) and entropy ($\Delta S^\ddagger = -35.5 \pm 1.3$ cal mol⁻¹ K⁻¹) of the reaction of DMD with cyclohexene which shows a reaction rate constant (0.462 L⁻¹ mol s⁻¹ in acetone at 25°C, $\Delta G^\ddagger = 17.7 \pm 0.4$ kcal mol⁻¹) very similar to that of cis-3-hexene. The difference between these values and our computational (gas phase) values (for cis-2-butene, Table 3) can be certainly attributed in part to solvation effects which should decrease both the

Table 4. Solvent effect on activation free enthalpy ($\delta\Delta G_{\text{sol}}^\ddagger$) and comparison between the corrected theoretical ($\Delta G_{\text{sol}}^\ddagger$ and $\Delta\Delta G_{\text{sol}}^\ddagger$) and experimental ($\Delta G_{\text{exp}}^\ddagger$ and $\Delta\Delta G_{\text{exp}}^\ddagger$) data.

TS	ΔG^\ddagger	$\delta\Delta G_{\text{sol}}^\ddagger$ ^a	$\Delta G_{\text{sol}}^\ddagger$ ^b	$\Delta\Delta G_{\text{sol}}^\ddagger$	$\Delta G_{\text{exp}}^\ddagger$	$\Delta\Delta G_{\text{exp}}^\ddagger$
2a	19.42	-5.89	13.53			
3a	20.42	-6.16	14.26			
4a	17.38	-6.17	11.21			
5a	19.62	-7.29	12.33			
6a	18.29	-6.76	11.53			
2b	24.93	-6.03	18.90	2.16 ^c	19.29	1.64
3b	26.49	-5.85	20.64			
4b	22.79	-6.08	16.71	0.00	17.65	0.00
6b	24.64	-6.54	18.10	1.39	18.91	1.26

^aElectrostatic solvent effect according to Tomasi model ($\epsilon = 21$) at the B3LYP/6-31G* level of theory. It is given as the difference between the solvent effect on the TSs and that on the reactants.

^b $\Delta G_{\text{sol}}^\ddagger$ includes the $\delta\Delta G_{\text{sol}}^\ddagger$ correction ($\Delta G_{\text{sol}}^\ddagger = \Delta G^\ddagger + \delta\Delta G_{\text{sol}}^\ddagger$)

^cContribution of both endo and exo pathways, i.e. **2b** and **3b**, to the reaction rate have to be considered for propene. This leads to $\Delta G^\ddagger = 18.87 \text{ kcal mol}^{-1}$ (see caption b of Table 3).

activation enthalpy and entropy. However, given that we cannot calculate solution ΔH^\ddagger and ΔS^\ddagger and due to fundamental uncertainty in comparing activation entropies for bimolecular reactions in the gas phase and solution⁴⁰, further discussion on this point is useless.

In conclusion, the Becke3-LYP/6-31G* level of theory predicts a symmetrical spiro butterfly TS with two identical C--O forming bond lengths for the reactions of the parent dioxirane and dimethyldioxirane with ethylene and cis-2-butene. In the case of propene and trans-2-butene the slight asynchrony in C--O bond formation is accompanied by a tilting of the dioxirane moiety as the result of electronic effects (double bond polarization) and/or steric effects. Calculated activation free enthalpies (both absolute and relative values) corrected for electrostatic solvation effects are in good accord with related experimental data suggesting that this level of theory is a reliable computational method to investigate this type of reactions.

Acknowledgement. Financial support from MURST and CNR is gratefully acknowledged.

REFERENCES AND NOTES

1. Curci, R.; Fiorentino, M.; Troisi, L.; Edwards, J. O.; Pater, R. H. *J. Org. Chem.* **1980**, *45*, 4758.
2. Murray, R. W.; Jeyarama, R.; Mohan, L. *Tetrahedron Lett.* **1986**, 2335.
3. Adam, W.; Curci, R.; Edwards, J. O. *Acc. Chem. Res.* **1989**, *22*, 205.
4. Curci, R.; Dinoi, A.; Rubino, M. F. *Pure Appl. Chem.* **1995**, *67*, 811.
5. Murray, R. W.; *Chem. Rev.* **1989**, *89*, 1187.
6. Adam, W.; Chan, Y. Y.; Cremer, D.; Gauss, J.; Scheutzow, D.; Schindler, M. *J. Org. Chem.* **1987**, *52*, 2800.
7. Adam, W.; Hadjiarapoglou, L.; Bialas, J.; *Chem. Ber.* **1991**, *124*, 2377.
8. Adam, W.; Hadjiarapoglou, L.; Bialas, J. *Topics in Current Chemistry* **1993**, *164*, 46.
9. Adam, W.; Paredes, R.; Smerz, A. K.; Veloza, L. A. *Liebigs Ann.* **1997**, 547-551.
10. Baumstark, A. I.; McCloskey, C. J. *Tetrahedron Lett.* **1987**, *28*, 3311 and references cited there.
11. Wang, Z.; Tu, Y.; Frohn, M.; Zhang, J.; Shi, Y. *J. Am. Chem. Soc.* **1997**, *119*, 11224.

12. Adam, W.; Smerz, A. K.; *J. Org. Chem.* **1996**, *61*, 3506.
13. Murray, R. W.; Hong Gu *J. Phys. Org. Chem* **1996**, *9*, 751.
14. Adam, W.; Smerz, A. K *Tetrahedron* **1995**, *51*, 13039.
15. Murray, R. W.; Singh, M.; Williams, B. L.; Moncrieff, H. M. *Tetrahedron Lett.* **1995**, *36*, 2437.
16. Murray, R. W.; Daquan Gu *J. J. Chem. Soc. Perkin Trans. 2* **1993**, 2203.
17. Kraka, E.; Konkoli, Z.; Cremer, D.; Fowler, J.; Schaefer III, H. F. *J. Am. Chem. Soc.* **1996**, *118*, 10595.
18. Gutbrod, R.; Schindler, R. N.; Kraka, E.; Konkoli, Z.; Cremer, D. *Chem. Phys. Lett.* **1996**, 252, 221.
19. Miaskiewicz, K.; Teich, N. A.; Smith, D. A. *J. Org. Chem.* **1997**, *62*, 6493.
20. Bach, R. D.; Andres, J. L.; Owensby, A. L.; Schlegel, H. B.; McDouall, J. J. W. *J. Am. Chem. Soc.* **1992**, *114*, 7207.
21. Singleton, D. A.; Merrigan, S. R.; Jian Liu, Houk, K. N. *J. Am. Chem. Soc.* **1997**, *119*, 3385.
22. Yamabe; S.; Kondou, C.; Minato, T. *J. Org. Chem.* **1996**, *61*, 616.
23. Bach, R. D.; Winter, J. L.; McDouall, J. J. W. *J. Am. Chem. Soc.* **1995**, *117*, 8586.
24. Gandolfi, R.; Freccero, M.; Sarzi-Amadè, M. to be submitted.
25. Gandolfi, R.; Sarzi-Amadè, M.; Rastelli, A.; Bagatti M.; *Tetrahedron Lett.* **1996**, *37*, 1321.
26. Houk, K. N.; Liu, J.; DeMello, N. C.; Condroski, K. R. *J. Am. Chem. Soc.* **1997**, *119*, 10147.
27. Jensen, C.; Liu, J.; Houk, K. N.; Jorgensen, W. L. *J. Am. Chem. Soc.* **1997**, *119*, 12982.
28. Becke, A. D. *J. Chem. Phys.* **1993**, *98*, 1372.
29. Lee, C.; Yang, W.; Parr, R.G. *Phys. Rev. B* **1988**, *37*, 785.
30. Gaussian 94; Frisch, M. J.; Trucks, G. W.; Schlegel, H. B.; Gill, P. M. W.; Johnson, B. G.; Robb, M. A.; Cheeseman, J. R.; Keith, T.; Peterson, G. A.; Montgomery, J. A.; Raghavachari, K.; Al-Laham, M. A.; Zakrzewski, V. G.; Ortiz, J. V.; Foresman, J. B.; Cioslowski, J.; Stefanov, B. B.; Nanayakkara, A.; Challacombe, M.; Peng, C. Y.; Ayala, P. Y.; Chen, W.; Wong, M. W.; Andres, J. L.; Replogle, E. S.; Gompert, R.; Martin, R. L.; Fox, D. J.; Binkley, J. S.; Defrees, D. J.; Baker, J.; Stewart, J. P.; Head-Gordon, M.; Gonzalez C.; Pople, J. A. Gaussian, Inc.: Pittsburgh, PA, 1995.
31. Rastelli, A.; Bagatti, M.; Gandolfi, R. *J. Am. Chem. Soc.* **1995**, *117*, 4965.
32. Miertus, S.; Tomasi, J. *J. Chem. Phys.* **1982**, *65*, 2392.
33. Miertus, S.; Scrocco, E.; Tomasi, J. *J. Chem. Phys.* **1981**, *55*, 117.
34. Coitino, E. L.; Tomasi, J.; Ventura, O. N. *J. Chem. Soc. Faraday Trans.* **1994**, *90*, 1745.
35. Tomasi, J.; Persico, M. *Chem Rev.* **1997**, *94*, 2027.
36. Bach, R. D.; Canepa C., Winter, J. L.; Blanchette P. E. *J. Org. Chem* **1997**, *62*, 5191.
37. Actually the exo TS of the reactions with 2-propen-1-ol suggests that both dioxirane oxygens are involved in hydrogen bonding (i.e., OH---O₁ = 2.17 Å and OH---O₂ = 2.70 Å in the most stable TS of the reaction with DHD). This hypothesis is also supported by the presence of substantial net negative charges on both dioxirane oxygens in the TSs of alkene epoxidation reactions (see, for example, later on)³⁸.
38. Gandolfi, R.; Freccero, M.; Sarzi-Amadè, M.; Rastelli, A. unpublished results.
39. The final very good accord between computational and experimental absolute values, which is certainly better than expected, should not be overemphasized. It might well be the result, at least in part, of accidental compensation of errors in evaluation of gas phase (Becke3-LYP parametrization and basis set used) and solvation energies (due to approximations in the Tomasi procedure). New data are necessary to confirm or disprove the excellent performance of DFT methods in evaluating absolute values.
40. Jorgensen W. L.; Lim, D.; Blake, J. F. *J. Am. Chem. Soc.* **1993**, *115*, 2936.